ELSEVIER

Applied Mathematical Modelling 25 (2001) 995–1013

APPLIED MATHEMATICAL MODELLING

www.elsevier.com/locate/apm

Fatigue crack growth under variable-amplitude loading: Part II – Code development and model validation ☆

Asok Ray *, Ravindra Patankar

Mechanical Engineering Department, The Pennsylvania State University, University Park, PA 16802, USA

Received 13 December 1999; received in revised form 25 January 2001; accepted 12 February 2001

Abstract

A state-space model of fatigue crack growth has been formulated based on the crack closure concept in the first part of the two-part paper. The unique feature of this state-space model is that the constitutive equation for crack-opening stress is governed by a low-order non-linear difference equation without the need for storage of a long load history. Therefore, savings in the computation time and memory requirements are significant. This paper, which is the second part, provides information for code development and validates the state-space model with fatigue test data for different types of variable-amplitude and spectrum loading in 7075-T6 and 2024-T3 aluminum alloys, respectively. Predictions of the state-space model are compared with those of the FASTRAN and AFGROW codes.

Keywords: Fatigue and fracture; State-space modeling; Random loading; Sequence effects

1. Introduction

The goal of this sequence of papers in two parts is to formulate and validate a non-linear dynamical model of fatigue crack growth in ductile alloys. The model must satisfy the following requirements:

1. Capability to capture the effects of single-cycle overload and underload, load sequencing, and spectrum loading.
2. Representation of physical phenomena of fracture mechanics within a semi-empirical structure.
3. Compatibility with dynamical models of operating plants for health monitoring and life extending control.
4. Validation by comparison with fatigue test data and other well-known code of fatigue crack growth.
5. Development and verification of a computer code using standard programming language(s).
6. Capability to execute the code in real-time on commercially available platforms such as PCs.

☆ The research work reported in this paper has been supported in party by National Science Foundation under grant no. CMS-9819074; National Academy of Sciences under a research fellowship award to the first author; ARINC Corporation under NASA Langley Research Center Cooperative Agreement No. NCC1-333.

* Corresponding author. Tel.: +1-814-865-6377; fax: +1-814-863-4848.
E-mail address: axr2@psu.edu (A. Ray).

0307-904X/01/$ - see front matter
PII: S0307-904X(01)00027-0

Nomenclature

A_k^j	parameter in the empirical equation of S_k^{oss} for $j = 1, 2, 3, 4$
a	crack length
C	parameter in the crack growth equation
E	Young's modulus
$F(\cdot, \cdot)$	crack length dependent geometry factor
$h(\cdot)$	crack growth function in crack growth equation
k	current cycle of applied stress
m	exponent parameter in the crack growth equation
m	number of cycles of a particular stress level in the load block
n	number of cycles of a particular stress level in the load block
R	stress ratio of minimum stress to maximum stress
S^{flow}	flow stress
$S^{\max}$	maximum stress within a cycle
$S^{\min}$	minimum stress within a cycle
S^{o}	crack opening stress
S^{oss}	crack opening stress under constant amplitude load given by empirical equation
S^{ult}	ultimate tensile strength
S^{y}	yield stress
t	specimen thickness
$U(\cdot)$	the heaviside function
w	half-width of center-cracked specimen or width of compact specimen
α	constraint factor for plane stress/strain
$\alpha^{\max}$	maximum value of α
$\alpha^{\min}$	minimum value of α
$\Delta a^{\max}$	crack increment above which $\alpha = \alpha^{\min}$
$\Delta a^{\min}$	crack increment below which $\alpha = \alpha^{\max}$
Δa_k	crack increment $(= a_k - a_{k-1})$
ΔK^{eff}	effective stress intensity factor range
ε^{thr}	positive lower bound for absolute value of maximum stress $\{S_k^{\max}, k \geqslant 0\}$
η	decay rate for S^{o}

A state-space model of fatigue crack growth has been formulated in the first part (which is the companion paper) to satisfy the above requirements. Since the state-space model is based on fracture-mechanistic principles of the crack closure concept, the requirements #1 and #2 are satisfied. The requirement #3 is also satisfied because the plant dynamic models are usually formulated in the state-space setting or autoregressive moving average (ARMA) setting [4].

This paper, which is the second part, builds upon the first part to satisfy the remaining three requirements #4, #5, and #6. Specifically, the state-space model is validated with fatigue test data for different types of variable-amplitude and spectrum loading on 7075-T6 and 2024-T3 aluminum alloys [5,9], respectively. The model predictions are also compared with those of FASTRAN [7] and AFGROW [1] codes. The FASTRAN code is well-known for fatigue crack growth prediction and has been widely used in the aircraft industry. The AFGROW code is an assimilation of recent fatigue crack growth packages including NASGRO that provides theoretical back-

ground of fatigue crack propagation behavior and details of the formulation used in the software. While the results derived from the state-space, AFGROW, and FASTRAN models are comparable, the state-space model enjoys significantly smaller computation time and memory requirements as needed for real-time execution on standard platforms such as a Pentium PC. This is because the state-space model is described by a low-order difference equation without the need for storage of a long load history. This simple structure of the state-space model facilitates the task of code generation and verification using standard programming languages. The information needed for development of a real-time computer code is provided in this paper.

This paper is organized in five sections. Section 2 rearranges the state-space model in a format that provides the information for development of a fatigue crack growth code. Section 2.4 validates the state-space model by comparison with fatigue test data under different types of variable amplitude loading including spectral loading for 7075-T6 and 2024-T3 aluminum alloys as well as with the predictions of the FASTRAN model and one of the AFGROW models under identical load excitation. Section 3 provides a comparison of execution time and memory requirements of the state-space model with those of the FASTRAN model. Section 4 summarizes and concludes both parts of the two-part sequence along with recommendations for future research.

2. Information for development of a fatigue crack growth code

The model equations derived in Part I [10] are now rearranged for developing a computer code of fatigue crack growth simulation. The main program of the code consists of three major segments: (i) *Parameter section* that defines the material and model parameters; (ii) *Initial section* that initializes the model by the static relationships as functions of the model parameters; and (iii) *Dynamic section* that recursively updates the state variables in response to the input excitation. The main program is supported by three *Function modules* that provide algebraic relationships to be used in the main program. The symbols in the equations below are the same as those used in the first part and are defined in the nomenclature.

2.1. Parameter section

Material parameters: S^{y}, S^{ult}, and E for the material under consideration are available in standard handbooks.

Model parameters: The parameter $\varepsilon^{thr} > 0$ provides the lower bound for absolute value of maximum stress $\{S_k^{max}, k \geqslant 0\}$.

The parameters $\alpha^{max}, \alpha^{min}, \ln(\Delta a^{max})$ and $\ln(\Delta a^{min})$ are used to evaluate the constraint factor α (see Fig. 1). Tables 1 and 2 list the parameters for 7075-T6 and 2024-T3 alloys. The FASTRAN manual [7] provides these parameters for different alloys.

Specimen geometry: For center-cracked specimens, half-width w and thickness t of the specimen are the key parameters.

2.2. Initial section

Parameter calculation:

$S^{flow} \equiv (S^{y} + S^{ult})/2$;

$\eta \equiv (tS^{y}/2wE)$ unless otherwise specified (e.g., based on experimental data of a specific configuration);

$\vartheta \equiv (\alpha^{max} - \alpha^{min})/(\ln(\Delta a^{min}) - \ln(\Delta a^{max}))$ for calculating the constraint factor α_k (see Fig. 1).

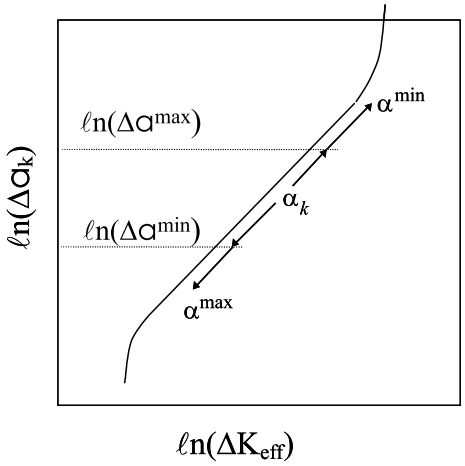

Fig. 1. Interpolation range for the crack growth curve.

Table 1
Crack growth lookup table for 7075-T6

ΔK^{eff} (MPa $\sqrt{\text{m}}$)	Crack growth rate (m/cycle)
0.90	1.0×10^{-11}
1.35	1.2×10^{-9}
3.40	1.0×10^{-8}
5.20	1.0×10^{-7}
11.9	1.0×10^{-6}
18.8	1.0×10^{-5}
29.0	1.0×10^{-4}

Table 2
Model parameters for fatigue crack growth in aluminum alloys

Alloy	$\alpha^{\max}$	$\alpha^{\min}$	$\Delta a^{\max}$	$\Delta a^{\min}$	C	m
7075-T6	1.8	1.1	5.0×10^{-6}	5.0×10^{-7}	Lookup table see Table 1	
2024-T3	1.73	1.1	7.5×10^{-7}	9.0×10^{-8}	5×10^{-11}	4.07

Model initialization: The initial peak and valley $\{S_0^{\max}, S_0^{\min}\}$ of the remote stress profile are given. Initial value a_0 of the crack length must be specified.

Specification of the initial value S_0^{o} is optional. If S_0^{o} is not specified, then it is estimated as:

$$S_0^{\text{o}} = S^{\text{oss}}(S_0^{\max}, S_0^{\min}, \alpha^{\max}, F(a_0, w), \varepsilon^{\text{thr}}).$$

2.3. Dynamic section

Input excitation profile: Peaks and valleys of the remote stress profile $\{S_k^{\max}, S_k^{\min}\},\ k = 1, 2, 3, \ldots$

Recursive relations for $k \geqslant 1$:

$F_k = F(a_{k-1}, w)$

if $(S_k^{\max} > S_{k-1}^0)$ then

$$\Delta K_k^{\text{eff}} = F_k \sqrt{\pi a_{k-1}} \left(S_k^{\max} - \max\right)\left(S_k^{\min}, S_{k-1}^0\right)$$

else

$$\Delta K_k^{\text{eff}} = 0$$

endif
$\Delta a_k = h(\Delta K_k^{\text{eff}})$
if $\Delta a_k > 0$ then

$\alpha_k = \alpha^{\max} + \big(\ln(\Delta a_k) - \ln(\Delta a^{\min})\big)\vartheta$
$\alpha_k = \min(\alpha_k, \alpha^{\max})$
$\alpha_k = \max\big(\alpha_k, \alpha^{\min}\big)$

else
$\alpha_k = \alpha^{\max}$
endif
$S_k^{\text{oss\_old}} = S^{\text{oss}}(S_k^{\max}, S_{k-1}^{\min}, \alpha_k, F_k, \varepsilon^{\text{thr}})$
$S_k^{\text{oss}} = S^{\text{oss}}(S_k^{\max}, S_k^{\min}, \alpha_k, F_k, \varepsilon^{\text{thr}})$
if $(S_k^{\text{oss}} \geqslant S_{k-1}^{\text{o}})$ then

$\Delta S_k^{\text{o}} = (S_k^{\text{oss}} - S_{k-1}^{\text{o}})$

else
if $(S_k^{\min} < S_{k-1}^{\min})$ then

$$\Delta S_k^{\text{o}} = \left(\frac{\eta}{1+\eta}\right)\left(S_k^{\text{oss}} - S_{k-1}^{\text{o}}\right) + \left(\frac{1}{1+\eta}\right)\left(S_k^{\text{oss}} - S_k^{\text{ass\_old}}\right)$$

else

$$\Delta S_k^{\text{o}} = \left(\frac{\eta}{1+\eta}\right)\left(S_k^{\text{oss}} - S_{k-1}^{\text{o}}\right)$$

endif
endif

$a_k = a_{k-1} + \Delta a_k$
$S_k^{\text{o}} = S_{k-1}^{\text{o}} + \Delta S_k^{\text{o}}$
$S_k^{\text{o}} = \max(S_k^{\text{o}}, 0)$

2.4. Function modules

Geometry factor function $F(a, w)$: Functional relations for geometry factors are given in the FASTRAN manual [7].

($F(a, w) = \sqrt{\sec(\{\pi/2\}\{a/w\})}$ for center-cracked specimens, for example)

Crack growth function $h(\Delta K^{\text{eff}})$: The non-negative function $h(\Delta K_k^{\text{eff}})$ in Eq. (1) of the first part is realized in either one of the following two ways:

- Lookup table (see Table 1) using the material-dependent tabulated data of $\ln(\Delta K_k^{\text{eff}})$ versus $\ln(h(\Delta K_k^{\text{eff}}))$.
- $h(\Delta K_k^{\text{eff}}) = C(\Delta K_k^{\text{eff}})^{\text{m}}$, where C and m are material-dependent constant parameters (see Table 2).

The FASTRAN manual [7] provides these parameters for different alloys.

Crack opening stress function $S^{\text{oss}}(S^{\max}, S^{\min}, \alpha, F, \varepsilon^{\text{thr}})$:
if $(S^{\max} < \varepsilon^{\text{thr}})$ then

$S^{oss} = 0$

else

$$R = \frac{S^{min}}{S^{max}}$$

$$A^0 = (0.825 - (0.34 - 0.05\alpha)\alpha)\left[\cos\left(\frac{\pi}{2}\frac{S^{max}F}{S^{flow}}\right)\right]^{1/\alpha}$$

$$A^1 = (0.415 - 0.071\alpha)\left(\frac{S^{max}F}{S^{flow}}\right)$$

if $(R > 0)$ then

$$A^3 = \left(2A^0 + A^1 - 1\right)$$
$$A^2 = \left(1 - A^0 - A^1 - A^3\right)$$

else

$A^3 = 0$

$A^2 = 0$

endif

$$S^{oss} = \left(A^0 + \left(A^1 + \left(A^2 + A^3R\right)R\right)R\right)S^{max}$$

endif

Based on the above information, a computer code for crack growth prediction may now be written using a standard programming language such as Fortran or C or C++.

3. Model validation with fatigue test data

This section validates the state-space model with the fatigue test data of: (i) 7075-T6 aluminum alloy specimens under different types of variable amplitude cyclic loading [9]; and (ii) 2024-T3 aluminum alloy specimens under spectrum loading [5], which are available in open literature. The state-space model predictions have been compared with those of FASTRAN [7] and several other crack-tip-plastic-zone-based models (e.g., Wheeler, Willenborg, and Chang) that are available in the AFGROW software package [1]. Of all the AFGROW models, predictions of the Walker equation with Willenborg retardation model are found to yield, on the average, closest agreement with the test data of McMillan and Pelloux as well as Porter. The predictions of the remaining AFGROW models are not presented in this paper as they do not convey any new information. The state-space, FASTRAN, and AFGROW models are compared with the test data in Figs. 2–11 and in Tables 4 and 5.

3.1. Validation of the state-space model with Porter data

Porter [9] collected fatigue test data on center-notched 7075-T6 aluminum alloy specimens made of 305 mm wide, 915 mm long, and 4.1 mm thick panels, for which $E = 69\,600$ MPa, $\sigma^y = 520$ MPa, and $\sigma^{ult} = 575$ MPa. The initial crack size ($2a$) was 12.7 mm and the experiments were conducted in laboratory air. Table 1 provides the lookup table data for $h(\cdot)$ in Section 2, which is used instead of the closed form expression $C(\Delta K_k^{eff})^m$, to generate predictions of both the

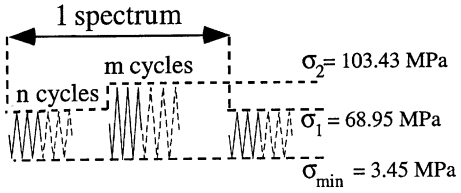

Fig. 2. Cyclic stress excitation for Porter data.

state-space and FASTRAN models. Table 2 lists the parameters of 7075-T6 aluminum alloy for updating the constraint factor α_k that varies between 1.1 and 1.8, depending on the instantaneous crack increment Δa_k [7, p. 62]. Fig. 2 shows the profile of block loading for data generation where the positive integers, n and m, indicate that a block of n constant-amplitude cycles is followed by a block of m cycles of a different constant-amplitude. Using the relationship $\eta \equiv (tS^y/2wE)$ in Section 2, the parameter η is evaluated to be $\sim 10^{-4}$ for the Porter specimen. Since η is stress-independent, this specific value is used for model validation under different loading conditions of Porter data.

Fig. 3 shows a comparison of the state-space model predictions with Porter data and the predictions of FASTRAN model and AFGROW (Walker equation with Willenborg retardation model) that calculate the crack opening stress S^o in a different way. The curves in each plate of Fig. 3 are generated with the parameter $n = 50$ and the peak stress of overload $\sigma_2 = 103.5$ MPa (15 ksi) at different values of m in the load spectrum of Fig. 2. The analyses on each of FASTRAN, AFGROW, and the state-space models have been conducted with identical initial crack length with the assumption of no loading history. Therefore, the initial value of S^o was not assigned.

The state-space and FASTRAN models produce essentially identical results under constant-amplitude cyclic stresses, because the procedure for calculation S^{oss} is similar in both models while the AFGROW model yields somewhat different results. For variable-amplitude cyclic stresses, the state-space model predictions are quite close to both the experimental data and predictions of the FASTRAN model, as seen in Fig. 3. Predictions of the three models are compared with Porter data in Fig. 4 for different amplitudes of overload with $m = 1$ and $n = 29$ (see Fig. 2) for different overload stress ratios σ_2/σ_1, while σ_1 is held fixed at 69 MPa (10 ksi). Similar comparisons are made in Fig. 5 for single-cycle overload (i.e., $m = 1$) with different values of overload spacing n and fixed values of $\sigma_2 = 103.5$ MPa (15 ksi) and $\sigma_1 = 69.0$ MPa (10 ksi). The plots in Figs. 4 and 5 indicate that the accuracy of the state-space model relative to the experimental data is comparable to that of the FASTRAN model. The state-space model appears to be less accurate than FASTRAN for overload–underload as seen in Fig. 6, and FASTRAN becomes less accurate for underload–overload in Fig. 7. In view of the fact that the test data are generated as an average of very few samples, the disagreements between the model predictions and the test data are not unreasonable.

On the average, for repeated overload and underload, accuracy of the state-space model is comparable to that of FASTRAN and AFGROW for the predictions displayed in Figs. 6 and 7. These results show that the state-space model (and, to lesser extent, FASTRAN) demonstrates the difference between the effects of overload–underload and underload–overload on crack growth in agreement with the test data. In contrast, the AFGROW model does not show any appreciable difference when corresponding results are compared. The predictions of the state-space model are apparently superior to those of AFGROW for sequence effects.

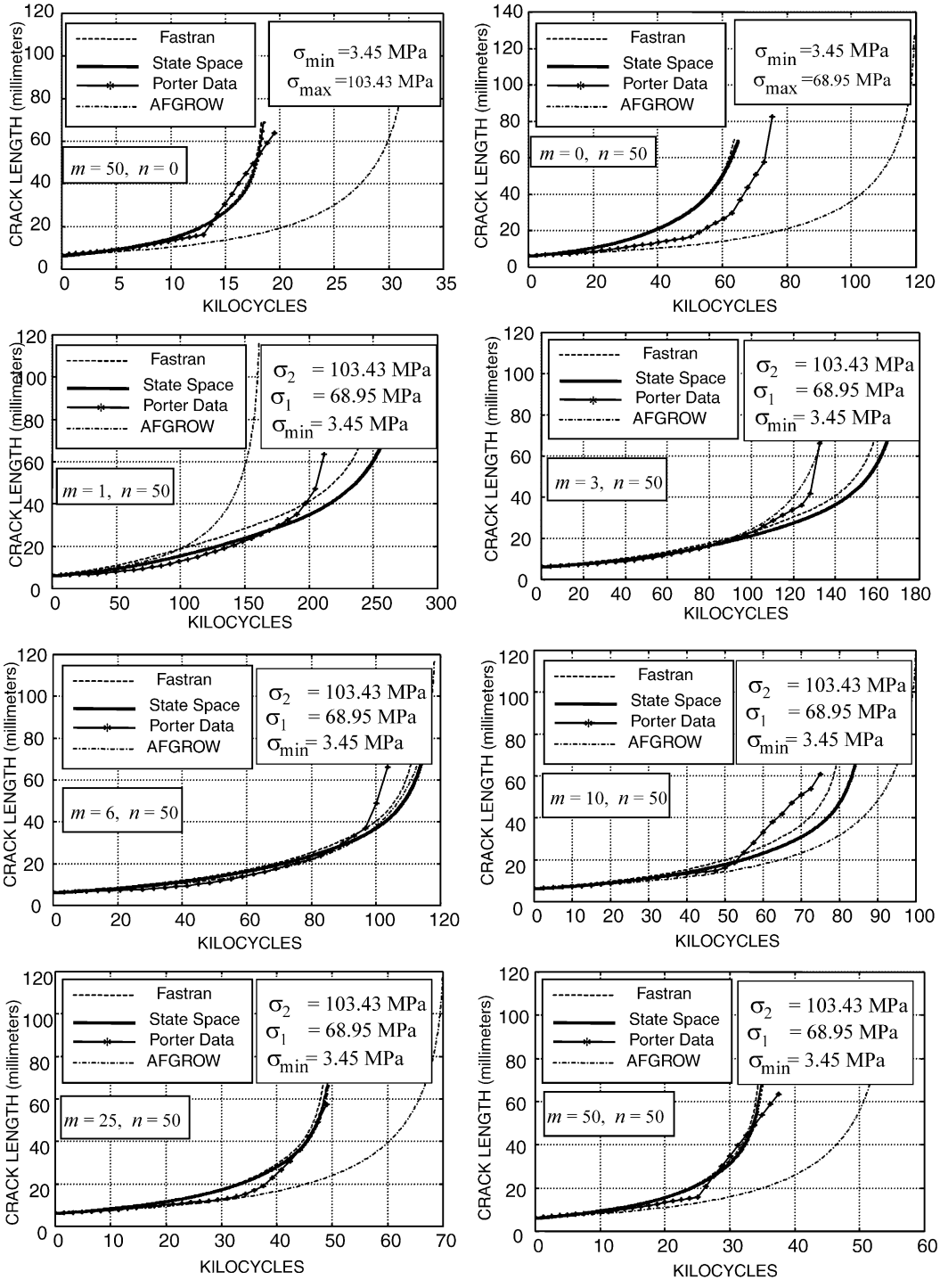

Fig. 3. Model validation with Porter data under block loading.

3.2. Predictions for complex spectrum loads

McMillan and Pelloux [5] collected fatigue data under complex spectrum loads for center-notched 2024-T3 aluminum alloy specimens made of 229 mm wide, 610 mm long, and 4.1 mm

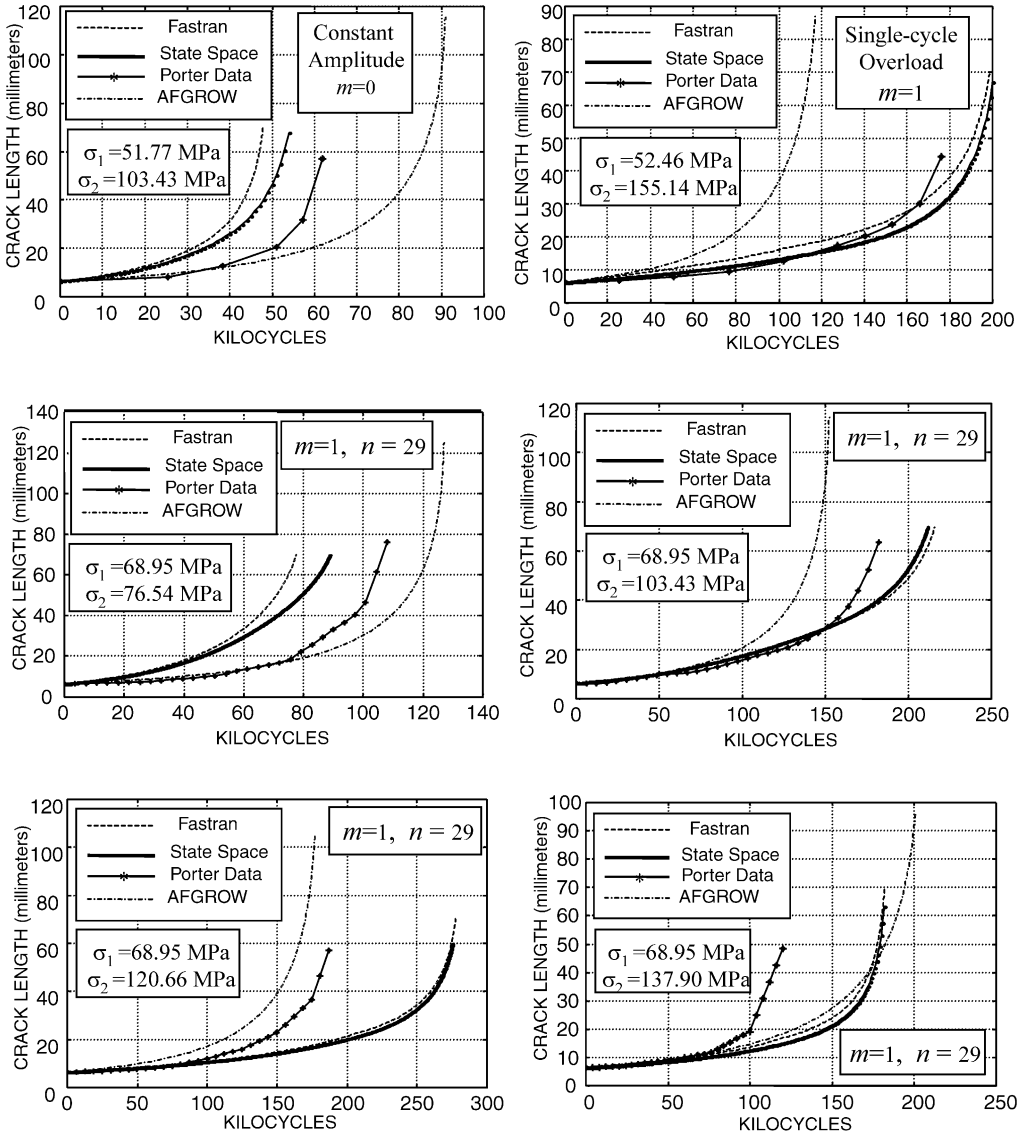

Fig. 4. Model validation with Porter data under different overload amplitude.

thick panels, for which $E = 71750$ MPa. Fatigue testing was accomplished in a vertical 125 kip electro-hydraulic fracture jig of Boeing design. The testing system was capable of applying loads with an absolute error within $\pm 1\%$ of the maximum programmed load. The initial crack size ($2a$) was 12.7 mm and the experiments were conducted in laboratory air. Thirteen load spectrum programs, P1–P13 were run on different specimen until failure. The composition of the 2024-T3 alloy used for spectra P1–P7 and P11–P13 was slightly different than the 2024-T3 alloy used for spectra P8–P10. The average properties of both materials based on three observations are listed in Table 3. Fatigue crack growth for spectra P1–P13 is calculated based on the parameters of 2024-T3 alloy in Table 2 and the closed form $C(\Delta K_k^{\text{eff}})^{\text{m}}$ of the function $h(\cdot)$ in Section 2. Using the relationship $\eta \equiv (tS^{\text{y}}/2wE)$ in Section 2, the parameter η is evaluated to be $\sim 0.78 \times 10^{-4}$ for spectra P8–P10 and $\sim 0.82 \times 10^{-4}$ for the remaining spectra based on the material parameters in Table 3.

Table 3
Average properties of 2024-T3 alloy used under load spectra young's modulus $E = 71\,750$ MPa for spectrum programs P1–P13

Spectrum program	Ultimate strength σ^{ult} (MPa)	Yield strength σ^{y} (MPa)
P1–P7, P11–P13	473.3	327.9
P8–P10	492.1	315.1

The predictions of the state-space and AFGROW models are very close to the majority of the 13 cases while FASTRAN predictions are apparently less accurate. The state-space model yields clearly better results than AFGROW for the test cases P7, P8, P11, and P12. However, AFGROW exhibits significantly better accuracy for a single test case P10. Predictions of the specimen life for the state-space and FASTRAN models are compared with test data of McMillan and Pelloux [5] for each load spectrum as shown in Table 4. Since the number of samples over which the test data are averaged is small (e.g., in the order of three or four), modest disagreements (in the range of $\sim$10%) between the state-space model predictions and the test data in Table 4 can be considered to be very good. Although all three models yield acceptable results, predictions of the state-space model are closest to the experimental data in 12 out of 13 cases of spectrum loads P1 through P13 as seen in the plates of Figs. 8–11. The agreement of model predictions with experimental data strongly supports the state-space model and its fundamental hypothesis that the crack opening stress can be treated as a state variable.

4. Comparison of computation time

Tables 5 and 6 list typical computation time required for calculation of crack growth under programmed loads for the Porter and McMillan and Pelloux data set, respectively, on a dual-

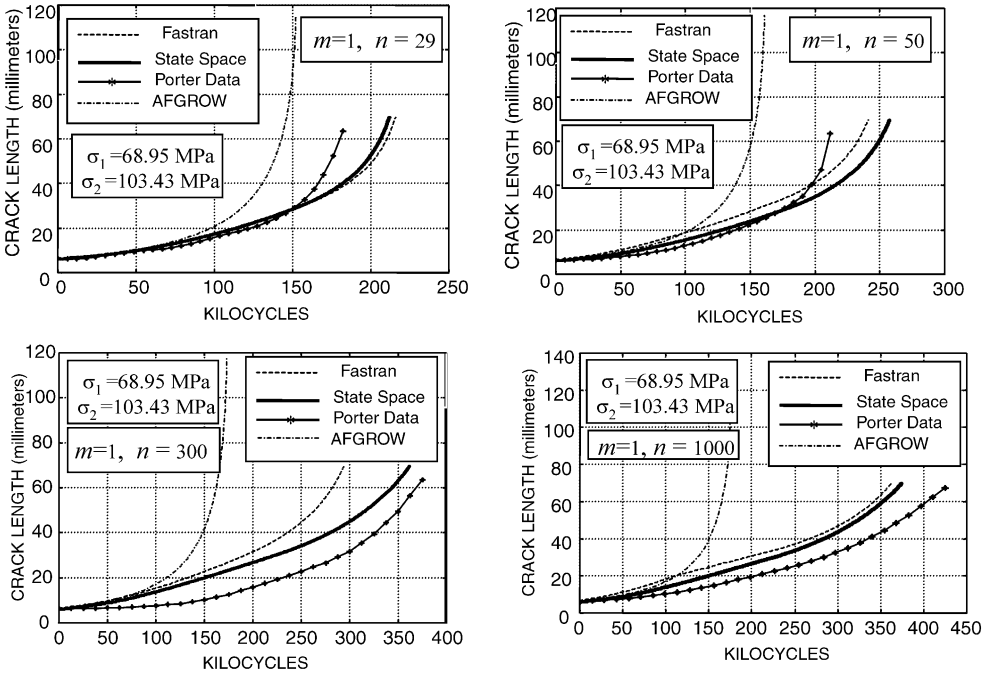

Fig. 5. Model validation with Porter data under different overload spacing.

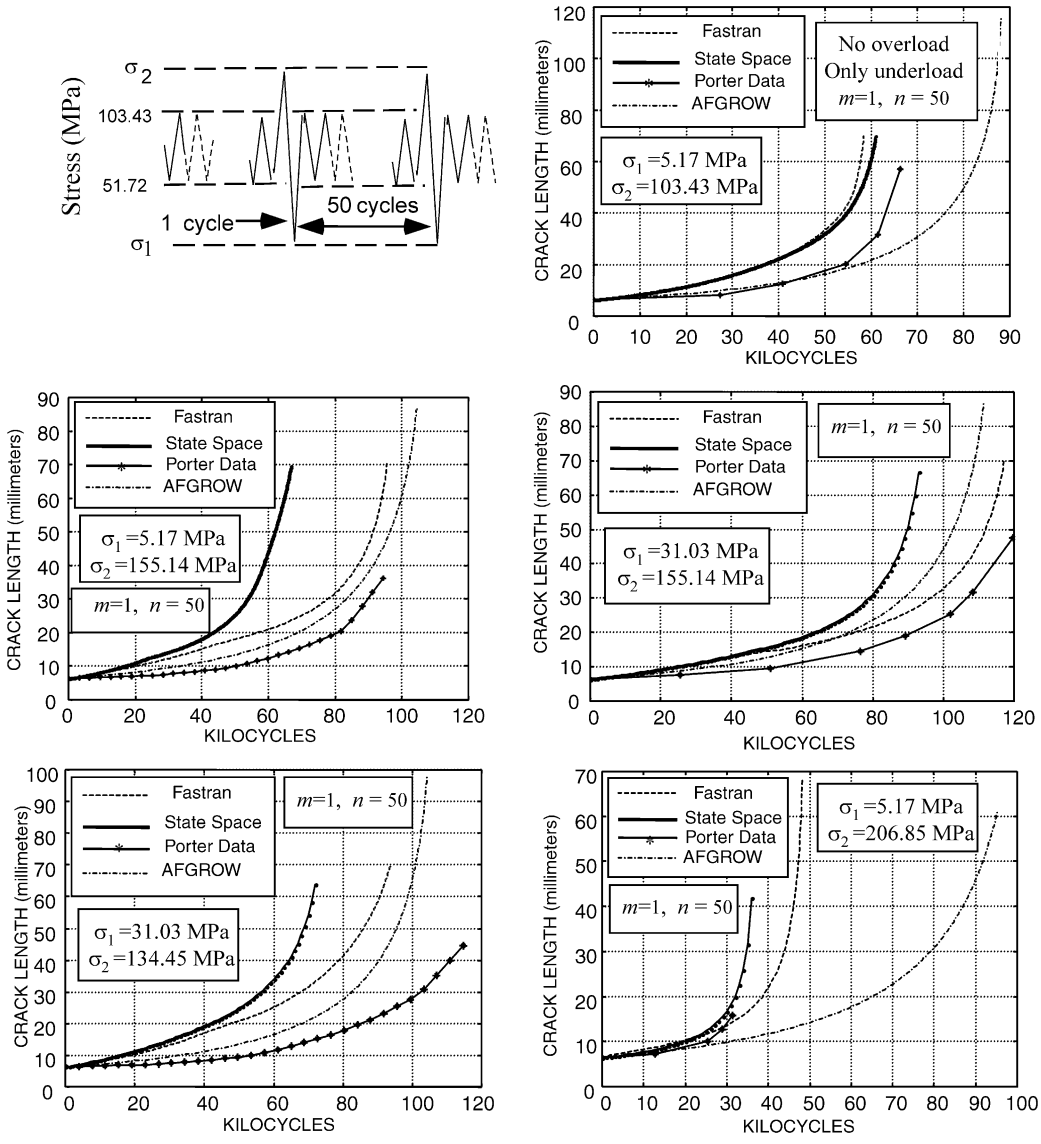

Fig. 6. Model validation with Porter data (overload–underload).

processor 450 MHz Intel Pentium PC platform. A similar comparison has been reported earlier by Patankar [8] on an SGI Indy platform. The actual execution time for AFGROW could not be assessed because the code involves a significant amount input/output operations including data writing and the source code is not available to the authors. In all of the 13 cases reported in Table 6, the state-space model predicts a longer life than FASTRAN. In the case of spectrum P10, the state-space and FASTRAN yield approximately similar number of cycles which provides a fair comparison of their computation time. Even though the life prediction of the state-space model is larger, its execution is more than 10 times faster than the FASTRAN model for the spectrum P10. The execution time per spectrum block for the cases P1–P13 indicates that the state-space model is at least 10 times faster than the FASTRAN model. The rationale for significantly enhanced computational performance of the state-space model is presented below.

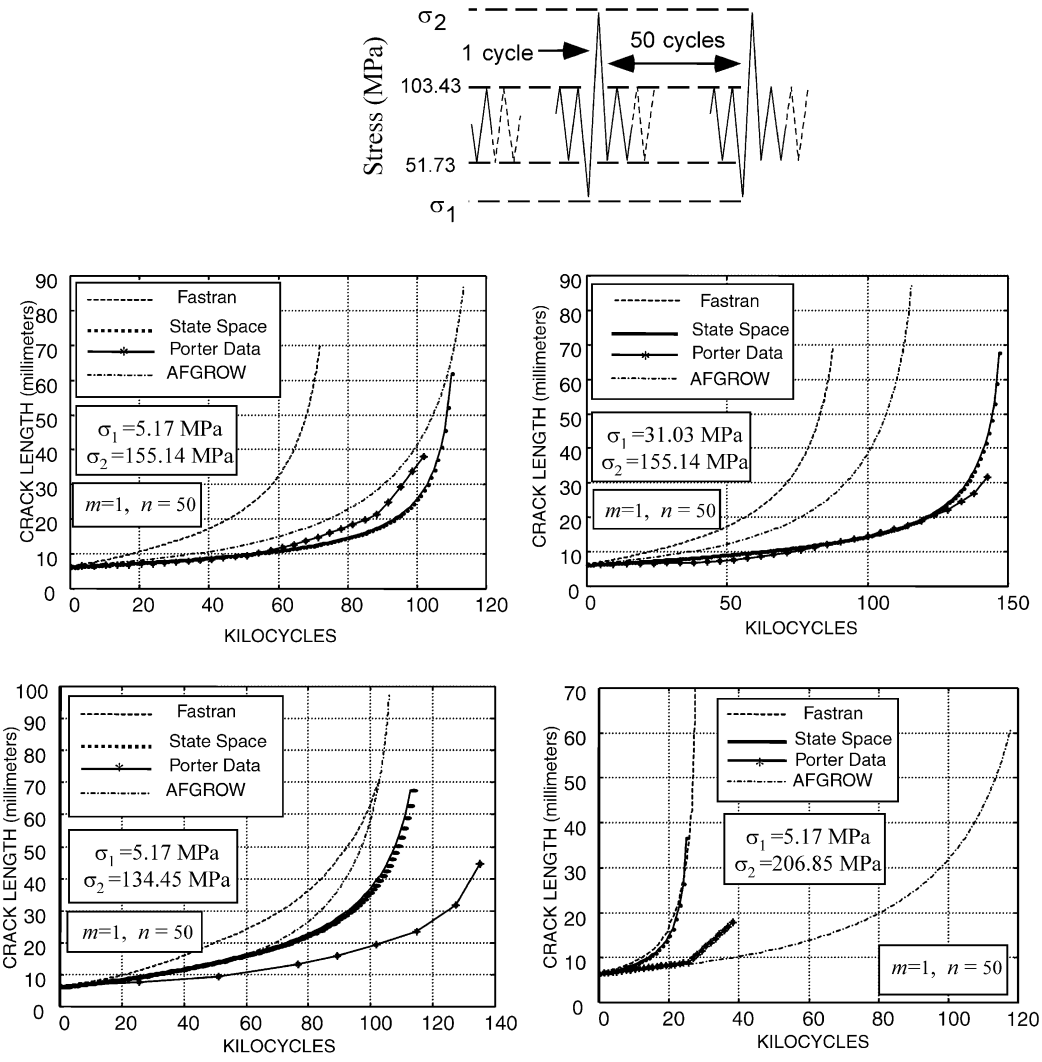

Fig. 7. Model validation with Porter data (underload–overload).

The state-space model recursively computes S_k^o with S_k^{max}, S_k^{min} and S_{k-1}^{max} as inputs, as seen in Section 2. This implies that the crack opening stress in the present cycle is obtained as a simple algebraic function of the maximum and minimum stress excitation in the present cycle as well as the minimum stress and the crack opening stress in the immediately preceding cycle. In contrast, the FASTRAN model computes the crack opening stress as a function of contact stresses and crack opening displacements based on the stress history.

Since the state-space model does not need storage of load history except the minimum stress in the previous cycle, its memory requirements are much lower than those of FASTRAN that does require storage of a relatively long load history. Consequently, both computer execution time and memory requirement of the state-space model are significantly smaller than those of FASTRAN. Specifically, the state-space enjoys the following advantages over other fatigue crack growth models:

- Smaller execution time and computer memory requirements as needed for real-time heath monitoring and life extending control [2].

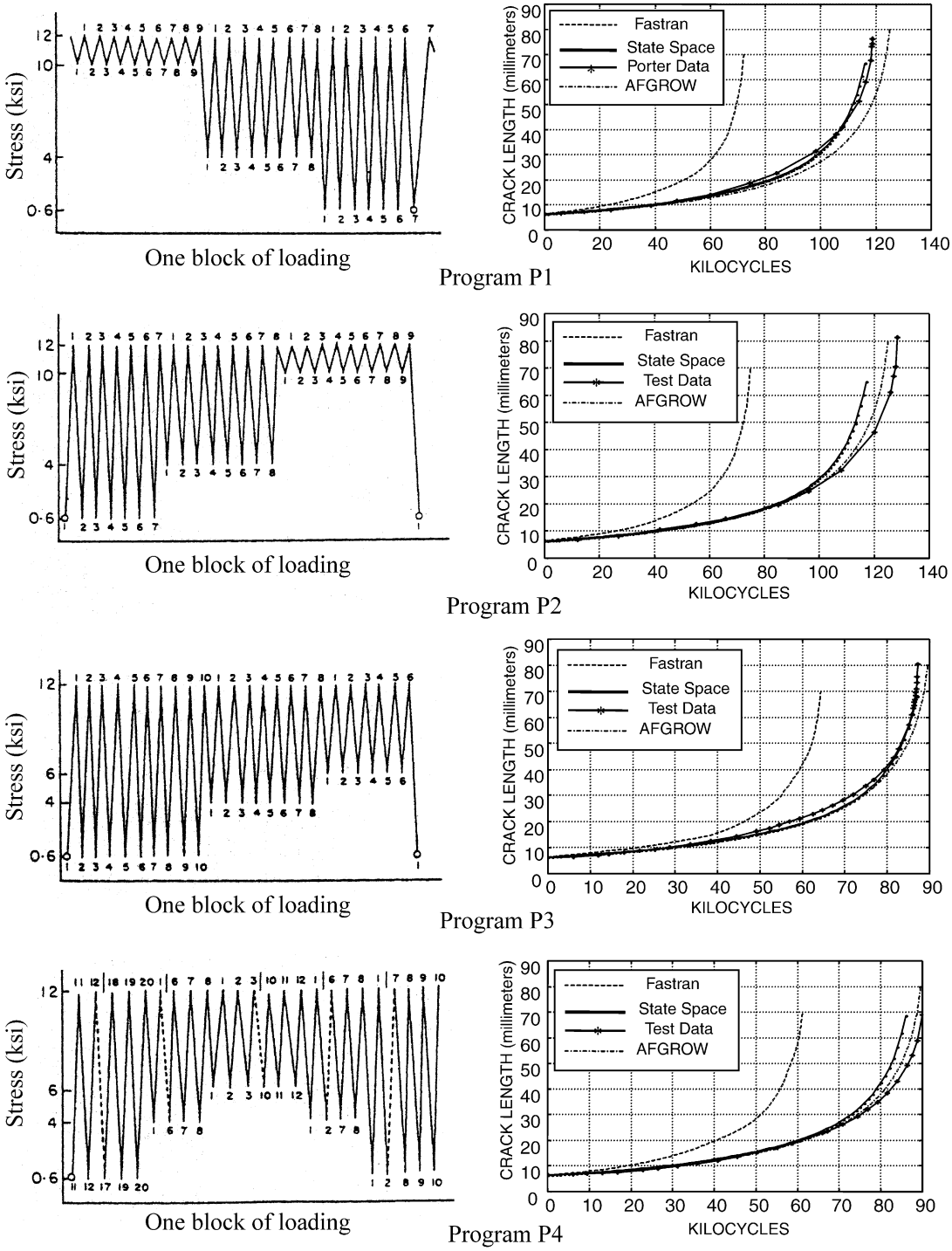

Fig. 8. Model validation with spectral data (programs P1–P4).

- Compatibility with other state-space models of plant dynamics (e.g., aircraft flight dynamic systems and rocket engine systems) and structural dynamics of critical components as needed for synthesis of life-extending control systems [2,3].

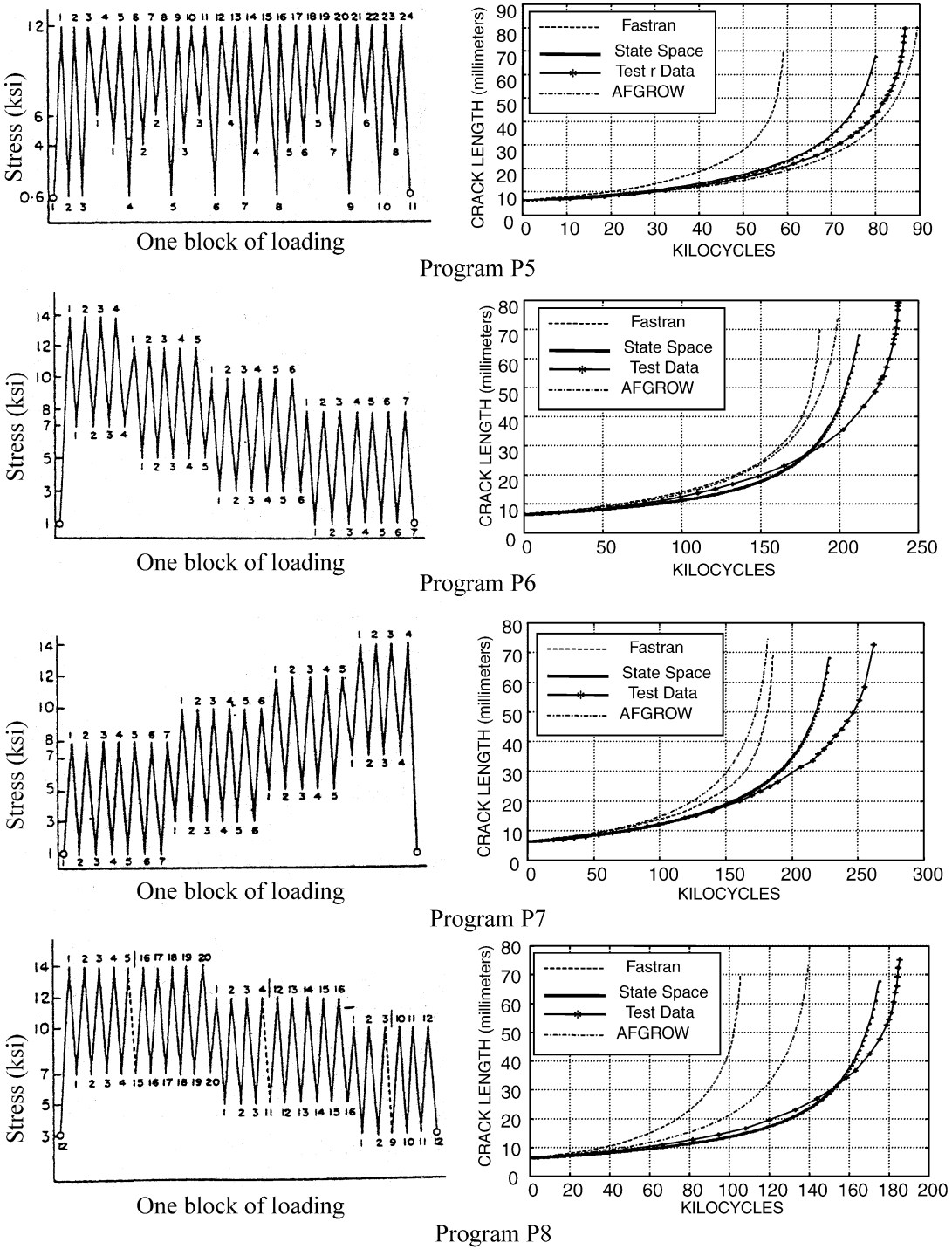

Fig. 9. Model validation with spectral data (programs P5–P8).

5. Summary, conclusions, and recommendations for future research

This section summarizes both parts of the two-part paper with pertinent conclusions on major advantages of the state-space model focusing on its usage for real-time applications. Topics for

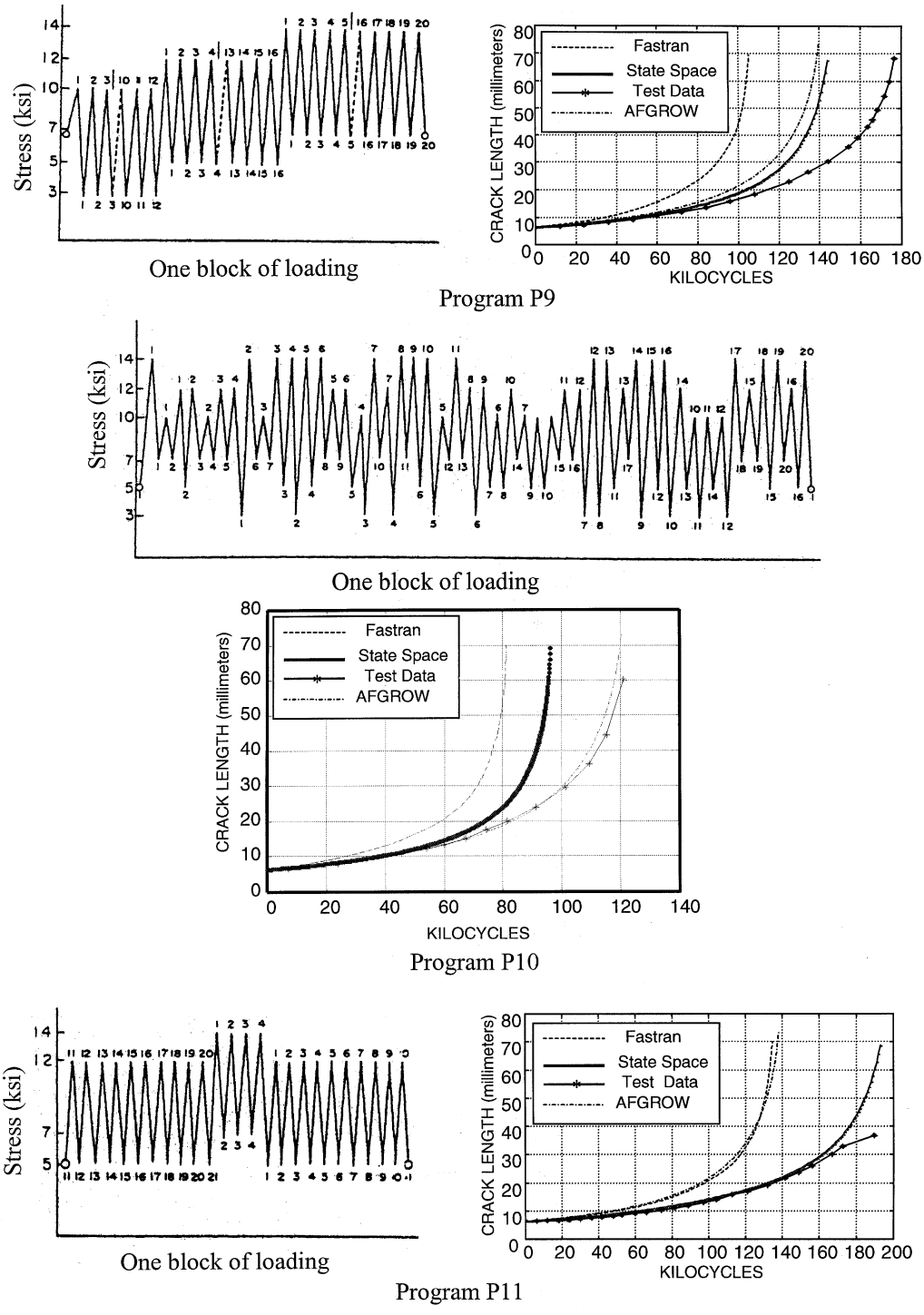

Fig. 10. Model validation with spectral data (programs P9–P11).

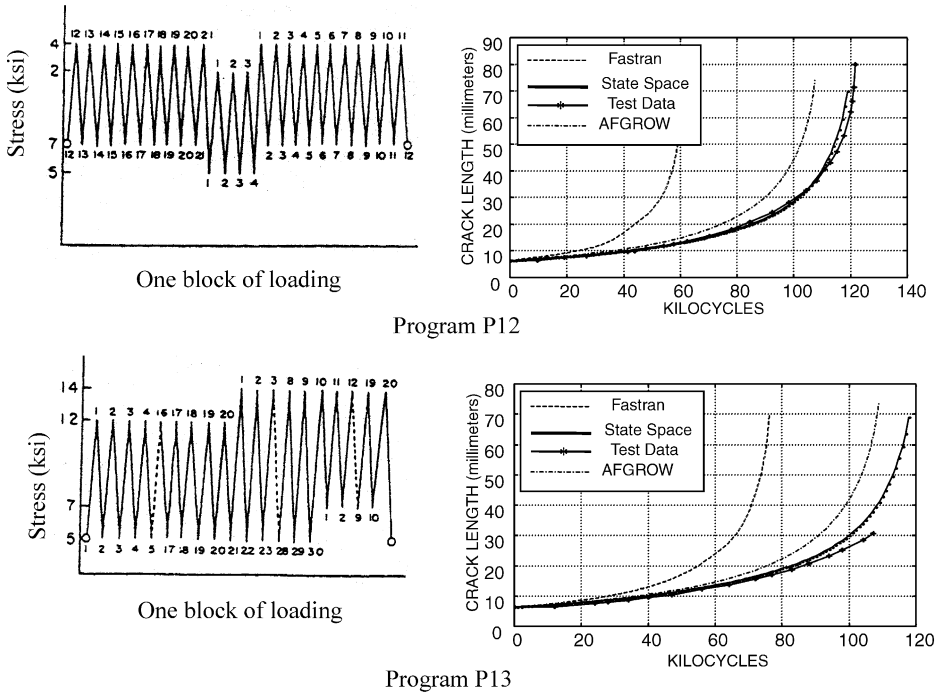

Fig. 11. Model validation with spectral data (programs P12–P13).

future research are also recommended to overcome some of the limitations and shortcomings of the state-space model.

5.1. Summary of the two-part paper

This two-part paper presents formulation and validation of a state-space model for fatigue crack growth prediction under variable-amplitude loading. The state-space model is built upon fracture-mechanistic principles of the crack-closure concept and experimental observations of

Table 4
Comparison of predicted and actual life under spectrum loads

Program spectrum	Specimen life in number of spectra			
	Test data	State-space model predictions	AFGROW model predictions	FASTRAN model predictions
P1	4950	4900	5650	3018
P2	5330	5000	5062	3135
P3	3630	3510	3641	2693
P4	1875	1690	1787	1282
P5	3605	3410	3736	2470
P6	10 775	9790	8697	8550
P7	11 900	9680	8267	8463
P8	3860	3780	2827	2211
P9	3700	2850	2721	2206
P10	2553	2010	2491	1691
P11	7900	7900	5150	5138
P12	5060	5000	3826	2560
P13	2680	2650	2198	1653

Table 5
Typical execution time of Porter data

Description of repeated load blocks	Execution time on a 450 MHz Pentium	
	State-space model predictions	FASTRAN model predictions
1000 cycles @ 68.95 MPa 1 cycle @ 103.43 MPa Minimum stress 3.45 MPa	1.20	4.80
300 cycles @ 68.95 MPa 1 cycle @ 103.43 MPa Minimum stress 3.45 MPa	1.10	4.50
50 cycles @ 68.95 MPa 1 cycle @ 103.43 MPa Minimum stress 3.45 MPa	0.50	2.30
1 cycle overload–underload @ 155.14 MPa–31.03 MPa 30 cycles constant-amplitude @ 103.43 MPa–51.72 MPa	0.30	3.50

Table 6
Execution time of Mcmillan and Pelloux data

Load description	State-space model (Time in seconds)	FASTRAN model (Time in seconds)
Program P1	0.65	4.09
Program P2	0.69	4.55
Program P3	0.50	5.70
Program P4	0.48	4.10
Program P5	0.47	5.07
Program P6	1.17	5.51
Program P7	1.28	5.10
Program P8	0.97	6.41
Program P9	0.79	7.16
Program P10	0.50	5.60
Program P11	1.07	5.36
Program P12	0.64	6.53
Program P13	0.66	5.31

fatigue test data. The model state variables are crack length and crack opening stress, and the model inputs are maximum stress and minimum stress in the current cycle and the minimum stress in the previous cycle. As such the crack growth model can be represented in the ARMA setting by a second-order non-linear difference equation that recursively computes the state variables without the need for storage of stress history except the minimum and maximum stresses in the present cycle and the minimum stress in the immediate past cycle. The two-state model can be augmented with additional states to capture the delayed effects of crack retardation if necessary.

Although the structure of the state-space model for crack growth prediction is similar to that of the FASTRAN model [7], the major difference is in the formulation of transient behavior of the crack opening stress. Since the crack opening stress in FASTRAN is calculated asynchronously based on a relatively long history of stress excitation over the past ($\sim$300) cycles, it does not follow a state-space structure. The state-space model of fatigue crack growth adequately captures the effects of stress overload and reverse plastic flow, and is applicable to various types of loading including single-cycle overloads, irregular sequences and random loads. The state-space model has been validated with fatigue test data of Porter [9] and McMillan and Pelloux [5] for 7075-T6 and 2024-T3, respectively. In the experimental data, the crack length a_k that is one of the state

variables is measurable. The other state variable, the crack-opening stress S^o, is determined from a finite history of the input (i.e., peaks and valleys of stress excitation) and the output (i.e., crack length measurements), starting from a particular cycle in the past onwards to the current cycle. The model predictions are also compared with those of FASTRAN and AFGROW for identical input stress excitation. While the results derived from these models are comparable, the state-space model enjoy significantly smaller computation time and memory requirements.

5.2. Pertinent conclusions

This state-space structure of the proposed fatigue crack growth model allows formulation of an ARMA model for real-time applications such as health monitoring and life extending control. Simplistic state-space models, meant for constant-amplitude loads [3], have been used earlier for monitoring and control applications because of unavilability of a reliable model for crack growth prediction under variable-amplitude load. With the availability of the state-space model, reliable strategies can now be formulated for real-time decision and control of damage-mitigation and life-extension.

5.3. Recommendations for future research

Although the constitutive equation for crack opening stress in the state-space model is built upon physical principles, the model formulation still relies on semi-empirical relationships derived from experimental data. More emphasis on the physics of fatigue fracture will enhance the credibility of the state-space model; and also expose its potential shortcomings, if any. Therefore, it is desirable to formulate the transient behavior of the crack opening stress in the microstructural setting based on the dislocation theory.

Currently, the transients of crack opening stress are estimated from the available fatigue test data of crack growth. The information on relatively fast dynamics of crack opening stress is likely to be contaminated during the estimation process. Transient test data on crack opening stress under load variations are necessary for identification of more accurate and reliable state-space models. Controlled experiments, equipped with high-bandwidth instrumentation, need to be carried out to determine the exact nature of non-linearities that are represented by the Heaviside functions in the state-space model. Availability of additional crack growth data, under different types of cyclic loads and for different materials and specimen geometry, will enhance validation of the state-space model.

The state-space model uses the structure of constant-amplitude crack opening stress [6] as a forcing function into the constitutive equation of crack opening stress. Construction of a state-space model based on other forcing functions needs to be explored. In addition, the dimensionless parameter η that determines the dynamical behavior of the crack opening stress S^o depends on the specimen material and geometry. The relationship $\eta = (tS^y/2wE)$ in Eq. (9) is obtained semi-empirically from the experimental data of center-cracked specimens of two alloys, 2024-T3 and 7075-T6, only. Further analytical research is needed to obtain a closed form relationship for the parameter η from experimental data on a variety of alloys under variable-amplitude load excitation.

Acknowledgements

The authors are grateful to Dr. James C. Newman, Jr. of NASA Langley Research Center for valuable technical consultations as well as for providing the FASTRAN code. The authors would

like to thank Dr. Gary Halford of NASA Glenn Research Center and Dr. Royce Forman of NASA Johnson Space Center for stimulating technical discussions. The first author acknowledges the assistance of Mr. V.V.S. Sastry in generation of model predictions.

References

[1] J.A. Harter, AFGROW Users' Guide and Technical Manual, Report No. AFRL-VA-WP-1999-3016, Air Force Research Laboratory, WPAFB, OH 45433-7542, 1999.
[2] M. Holmes, A. Ray, Fuzzy damage mitigating control of mechanical structures, ASME J. Dyn. Syst., Meas. Control 120 (2) (1998) 249–256.
[3] C.F. Lorenzo, M. Holmes, A. Ray, Design of life extending control using nonlinear parameter optimization, Lewis Research Center Technical Report No. NASA TP 3700, 1998.
[4] L. Ljung, System Identification Theory for the User, second ed., Prentice-Hall, Englewood Cliffs, NJ, 1999.
[5] J.C. McMillan, R.M.N. Pelloux, Fatigue crack propagation under program and random loads, fatigue crack propagation, ASTM STP 415 (also Boeing Space Research Laboratory (BSRL) Document D1-82-0558, 1996), 1967, pp. 505–532.
[6] J.C. Newman Jr., A crack opening stress equation for fatigue crack growth, Int. J. Fract. 24 (1984) R131–R135.
[7] J.C. Newman Jr., FASTRAN-II – A fatigue crack growth structural analysis program, NASA Technical Memorandum 104159, Langley Research Center, Hampton, VA 23665, 1992.
[8] R. Patankar, Modeling fatigue crack growth for life extending control, Doctoral Dissertation in Mechanical Engineering, The Pennsylvania State University, University Park, May 1999.
[9] T.R. Porter, Method of analysis and prediction for variable amplitude fatigue crack growth, Eng. Fract. Mech. 4 (1972) 717–736.
[10] A. Ray, R. Patankar, Appl. Math. Modelling 25 (2001) 979–994, Part I.